Mantle earthquakes frozen in mylonitized ultramafic pseudotachylytes of spinel-lherzolite facies

T. Ueda*[1], M. Obata[1], G. Di Toro[2], K. Kanagawa[3], K. Ozawa[4]
[1]Division of Earth and Planetary Sciences, Graduate School of Science, Kyoto University, Kitashirakawa Oiwakecho, Sakyo-ku, Kyoto 606-8502, Japan
[2]Dipartimento di Geoscienze, Padova University, Via Giotto 1, 35317 Padova, Italy, and Istituto Nazionale di Geofisica e Vulcanologia, Via di Vigna Murata 605, 00143 Rome, Italy
[3]Department of Earth Sciences, Chiba University, 1-33 Yayoi-cho, Inage-ku, Chiba 263-8522, Japan
[4]Department of Earth and Planetary Sciences, Graduate School of Science, University of Tokyo, 7-3-1 Hongo, Bunkyo-ku, Tokyo 113-0033, Japan

ABSTRACT

We report a new type of ultramafic pseudotachylyte that forms a fault- and injection-vein network hosted in the mantle-derived Balmuccia peridotite (Italy). In the fault vein the pseudotachylyte is now deformed and recrystallized into a spinel-lherzolite facies ultramylonite, made of a fine (<2 m) aggregate of olivine, orthopyroxene, clinopyroxene, and spinel, with small amounts of amphibole and dolomite. Electron backscattered diffraction study of the ultramylonite shows a clear crystallographic preferred orientation (CPO) of olivine. The fault vein pseudotachylyte overprints a spinel-lherzolite facies amphibole-bearing mylonite, indicating that shear localization accompanying chemical reaction had taken place in the peridotite before seismic slip produced frictional melting. The occurrence of amphibole in the host mylonite and that of dolomite as well as amphibole in the matrices of ultramylonite and pseudotachylyte may indicate that fluid was present and had evolved in its composition from H_2O-rich to CO_2-rich during ductile deformation with metamorphic reactions, which may account for the observed rheological transition from ductile to brittle behavior. The spinel-lherzolite facies assemblage in mylonites, *P-T* estimations from pyroxene geothermometry and carbonate reactions, and the type of olivine CPO in deformed pseudotachylyte indicate that both the preseismic and the postseismic ductile deformations occurred at ~800 °C and 0.7–1.1 GPa.

Keywords: pseudotachylyte, mantle, peridotite, mylonite, shear localization, earthquake, fluid, dolomite, Balmuccia, Ivrea zone.

INTRODUCTION

Shear-induced rock melting during earthquakes may occur at mantle depths, according to torsion experiments conducted under high confining pressure (Bridgman, 1936) and theoretical studies (e.g., Griggs and Handin, 1960). Kanamori et al. (1998) assumed extensive production of seismic melts during the Mw = 8.3 Bolivian 1994 deep-focus (~600 km in depth) earthquake to justify its low seismic efficiency. The product of solidification of seismic melts is pseudotachylyte, which allows us to study the earthquake source mechanics complementary to the conventional seismological method (e.g., Sibson, 1975; Di Toro et al., 2005).

Ultramafic pseudotachylytes decorate exhumed faults cutting the subcontinental peridotite lenses of Balmuccia (Obata and Karato, 1995) in Italy and the oceanic peridotites in Corsica (Andersen and Austrheim, 2006). Common to these ultramafic pseudotachylytes is the presence of microlites in a glassy matrix (Obata and Karato, 1995; Andersen and Austrheim, 2006). In contrast to the ultramafic pseudotachylytes previously described from the same (Obata and Karato, 1995) and other areas, this study shows evidence for high-temperature mylonitization (in the spinel-lherzolite facies, ~800 °C) of pseudotachylytes, among the highest ever reported. The sequence of events inferred from structural and mineralogical observations supports the possibility of frictional melting and will provide constraints on earthquake nucleation at mantle depths.

GEOLOGIC SETTING

The Balmuccia peridotite is a lenticular mass of spinel lherzolite of 5 × 0.8 km in size, which is enclosed in an upper amphibolite to granulite facies mafic terrain—the Ivrea zone, northern Italy (see Fig. 1 of Obata and Karato, 1995; the geologic map is also in the GSA Data Repository Fig. DR1[1]). The main lithology of the peridotite massif is spinel lherzolite and spinel harzburgite with porphyroclastic to granoblastic textures (e.g., Rivalenti et al., 1981; Sinigoi et al., 1983). Layers or dikes of pyroxenite are locally abundant, some of which are folded and cut by faults associated with pseudotachylytes. The peridotite was primarily equilibrated in the mantle at temperature and pressure conditions of 1100 °C < *T* < 1200 °C and 1.3 GPa < *P* < 2.0 GPa, respectively (Shervais, 1979). Tectonic emplacement of the peridotite into the continental crust took place during the Carboniferous at 300–320 Ma and was accompanied by high-grade metamorphism at 720 °C < *T* < 900 °C and 0.9 GPa < *P* < 1.1 GPa (Schmid and Wood, 1976; Handy et al., 1999). The peridotite–mafic granulite complex was first exhumed during the Permian transtension and the early Mesozoic rifting of the Piedmont Ligurian Ocean (Handy and Stünitz, 2002) and then involved in the Tertiary brittle deformation along the Insubric Line during the Alpine collision (Handy et al., 1999).

HOST PERIDOTITES AND PSEUDOTACHYLYTES

Pseudotachylytes, as commonly observed elsewhere (Sibson, 1975), occur as both fault veins and injection veins, locally forming complex networks in the Balmuccia peridotite. The pseudotachylyte fault veins are typically 1–10 mm thick, straight, and appear black and glassy on fresh surfaces and light yellow on weathered surfaces (see photos in Fig. DR2). At the banks along the Sesia River (45°49′12″N, 8°09′12″E), the fault veins are subvertical and strike ~020° and 340°. The sense of shear and finite displacement on these faults may sometimes be determined by the offset of the pyroxenite bands (Fig. 2 in Jin et al., 1998).

Host Peridotites

The host rock, away from fault veins, is protogranular coarse-grained spinel lherzolite (with average modal composition, olivine [~60%], orthopyroxene [~25%], clinopyroxene [~10%], and Cr-Al spinel [~5%]; Obata and Karato, 1995). Approaching the fault, wall rocks are progressively deformed and recrystallized (Jin et al., 1998): They form a protomylonite-mylonite consisting of plastically deformed porphyroclasts of olivine, pyroxene, and

*E-mail: t_ueda@kueps.kyoto-u.ac.jp

[1]GSA Data Repository item 2008147, Figure DR1 (geologic map), Figure DR2 (field photographs of fault vein pseudotachylytes), Figure DR3 (photomicrograph showing deflection of the structure of host peridotite [sample 9310]), Figure DR4 (color version of Figure 3), and Table DR1 (microprobe analyses of mineral), is available online at www.geosociety.org/pubs/ft2008.htm, or on request from editing@geosociety.org or Documents Secretary, GSA, P.O. Box 9140, Boulder, CO 80301, USA.

spinel immersed in a fine-grained (10–50 m) matrix of recrystallized olivine, orthopyroxene, clinopyroxene, spinel, and pargasitic amphibole (Fig. 1A). Within ~20 cm of the fault, the porphyroclasts are elongated and deflected toward the fault (see a photomicrograph in Fig. DR3). Electron microprobe analyses show that recrystallized neoblastic pyroxenes are distinctly less aluminous than the porphyroclastic ones, while olivine is homogeneous ($Fo_{89–90}$) throughout (Table DR1, Fig. DR4). The amphibole is titaniferous pargasite and typically occurs in fine-grained parts (<60 m, neoblasts) along grain boundaries of primary large crystals of olivine and pyroxenes.

Pseudotachylyte Fault (i.e., Ultramylonite) and Injection Veins

The fault vein pseudotachylyte is foliated and mylonitized into a fine-grained (<2 m) polymineralic matrix and is formally "ultramylonite" (Fig. 1A). The contact between the wall rock mylonite and the ultramylonite is typically sharp because of the abrupt reduction in grain size and the color contrast (the pseudotachylyte-derived ultramylonite being more brownish in transmitted light; Fig. 1C). Some porphyroclasts in the host mylonite are truncated by the ultramylonite fault vein (Fig. 1A). The ultramylonite contains porphyroclasts of olivine, spinel, orthopyroxene, and clinopyroxene. The sense of shear deduced from the δ-type porphyroclasts (e.g., dextral in Fig. 1B) in the fault vein is consistent with that deduced from dike separations, with shape-preferred orientation (SPO) in the ultramylonite matrix and with the deflection in the host mylonite.

The presence of an injection vein connected to the main ultramylonite shear band (Fig. 1C; Fig. DR2) does suggest that the ultramylonite was originally a pseudotachylyte of melt origin. While the main shear zone is foliated, the injection and the pockets are largely massive but locally contain a weak foliation defined by the alignment of elongated olivine clasts, subparallel to the injection wall and at high angles to the main fault vein.

Scanning electron microscope (SEM) investigations of the pseudotachylyte revealed that both the fault and injection vein materials are holocrystalline, very fine-grained (<2 m) and equigranular to subequigranular, consisting of olivine, orthopyroxene, clinopyroxene, and spinel, with small amounts (a few volume percent) of amphibole and dolomite. Dolomite and amphibole were identified by a combination of electron backscattered diffraction (EBSD) pattern and semiquantitative X-ray spectroscopy. Dolomite is ubiquitous in the pseudotachylyte, both in the fault vein and in the injection vein; it appears as the dark phase in backscattered electron (BSE) images (Figs. 2A and 2B). An accurate modal amount of the amphibole is difficult to estimate in BSE images but is probably less than a few percent according to EBSD analysis and compositional mapping by X-ray spectroscopy. Olivine, pyroxene, amphibole, and dolomite are texturally and thus chemically in equilibrium (Fig. 2A). In addition, the injection veins contain numerous nanoparticles of Fe-Ni sulfide (as identified by energy-dispersive X-ray spectroscopy [EDS]) along the grain boundaries, while the sulfide grains are sparse and coarser-grained in the mylonitized fault vein. A shape-preferred orientation (SPO) was observed in an injection vein at high magnification (Fig. 2A). The lack of obvious SPO in the fault vein may be ascribed to more extensive recrystallization during the postseismic shear. The SPO is subparallel to the wall of the injection vein and at high angles to the fault vein. Furthermore, the fault vein has a clear crystallographic preferred orientation (CPO) of olivine as described below.

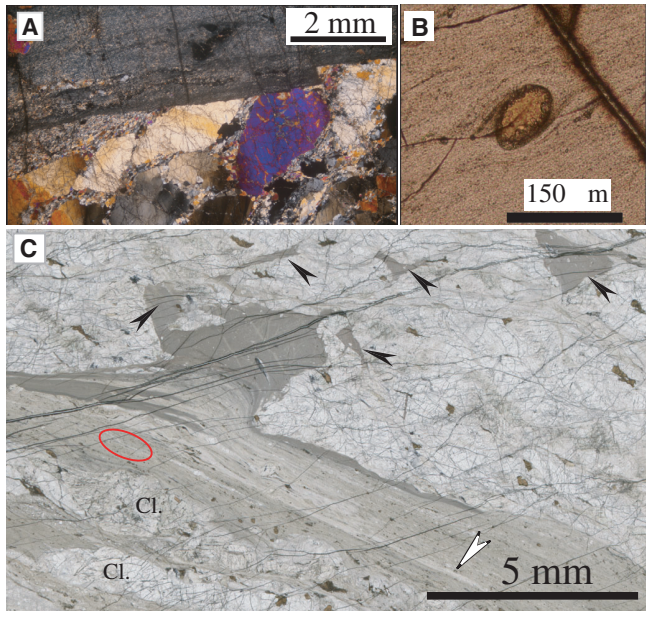

Figure 1. Optical images of the mylonitized pseudotachylyte. A: The wall rock protomylonite (bottom) truncated by the ultramylonite (= mylonitized pseudotachylyte fault vein, top). Cross-polarized light. B: Porphyroclastic system of spinel in the mylonitized pseudotachylyte. The wings of stable spinel indicate high-temperature deformation during postseismic deformation (see text). Fault plane is horizontal. Plane-polarized light. C: Injection vein and pockets (black arrows) originated from mylonitized pseudotachylyte fault vein. Pseudotachylyte pockets probably connected to the fault vein, judging from observation of multiple thin sections of the same sample. Thin white "ribbon" (white arrow) in the fault vein is elongated tail of clasts. Light-colored thick bands labeled "Cl." are slices of host protomylonite. Red ellipse indicates the layer from which CPO data (Fig. 3) were obtained. Sinistral shear. Plane-polarized light. Sample VS14.

CRYSTALLOGRAPHIC PREFERRED ORIENTATION (CPO) OF OLIVINE

Crystallographic orientations of olivine in the fault vein pseudotachylyte (i.e., ultramylonite) were studied using the EBSD technique. Measurements were made on a thin section cut orthogonal to the fault foliation and parallel to the lineation, using a JEOL JSM-6460 SEM (Chiba University) and a JEOL 7000F FE-SEM (University of Tokyo) operating at 15–20 kV and 5–9 nA. Data were processed using HKL Channel-5 software (Flamenco). Because of the small grain size (mostly less than 1 m in diameter), indexing of electron diffraction pattern together with phase identification was

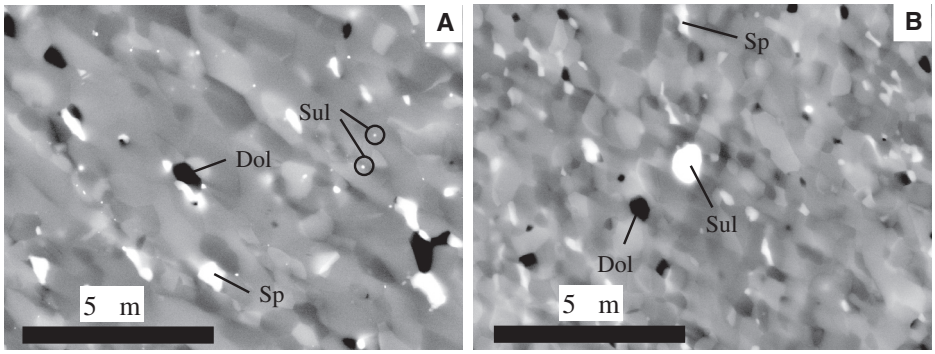

Figure 2. BSE image of an injection vein (A) and a fault vein pseudotachylyte (B) (sample VS14) obtained at 15 keV. The direction of the fault plane is parallel to the short side of photographs. Dol—dolomite; Sp—spinel; Sul—sulfide.

made manually on each beam spot. The results are plotted in Figure 3.

Olivine exhibits a CPO with [100] axes subparallel to the lineation and [010] axes subperpendicular to the foliation (Fig. 3) rather similar to the A-type fabric of Jung and Karato (2001), which may indicate an activation of the (010)[100] slip system in olivine (Carter and Avé Lallemant, 1970), suggesting a significantly high-temperature ductile deformation within the fault vein.

The host, coarse-grained peridotite, remote from the fault vein, also has the A-type CPO pattern, but with a distinct orientation of maxima from that of the mylonitized pseudotachylyte (see Fig. 8 in Jin et al., 1998). The olivine CPO of protomylonite becomes diffuse as the fault is approached, a result of the recrystallized fine-grained olivine having a different CPO pattern from the porphyroclasts as seen in Figure 8B of Jin et al. (1998), i.e., a strong [001] maximum and diffuse [100] and [010] peaks. The latter is distinct from the CPO we observed in the mylonitized pseudotachylyte.

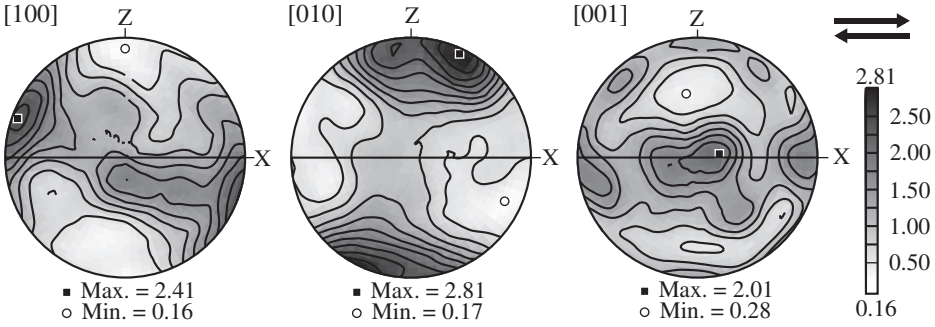

Figure 3. Pole figures of crystallographic orientations of olivine (axes [100], [010], and [001]) in a mylonitized pseudotachylyte, obtained by EBSD. The data were obtained from another thin section of the same sample (VS14); red ellipse in Figure 1C indicates the relevant layer from which the EBSD data were obtained. Foliation is horizontal (XY plane, solid line) with lineation (X). The shear sense is indicated by arrows on the top right. Equal-area, lower-hemisphere projections. The gray shading is calculated with Gaussian half-width of 15° referring to the density of data points (n = 164); the numbers in the legend are the multiples of uniform distribution density. A color version of the same diagram is given in Fig. DR4 (see footnote 1).

DISCUSSION

Sequence of Deformation and Crystallization Events

From textural observation the sequence of events in the shear zone is inferred as follows: (1) shear localization and recrystallization of host peridotite (that involve hydration, i.e., the amphibole formation), producing a narrow mylonite zone, (2) a seismic rupture and slip in or around the mylonite zone, which resulted in frictional melting and the formation of pseudotachylyte, and (3) a further shear *within* the pseudotachylyte vein, producing an ultramylonite. The deflection of the ultramylonite foliation at the mouth of the injection vein (Fig. 1C) may indicate that flowing material was still hot and fluidal during a residual shear of the main seismic slip and melting. The high-temperature CPO (Fig. 3) is consistent with this inference. Petrological and mineralogical observations indicate that this sequence of event took place under spinel-lherzolite facies conditions.

The preseismic ductile shear that produced the host mylonite was probably a slow and long-lasting ductile deformation event, because the dominant mechanism of the deformation is thought to be the dislocation creep coupled with metamorphic reactions, which are governed by diffusive processes both in the solid and along grain boundaries. Seismic rupture, on the other hand, involves rapid displacement (of the rate 1–5 m/s) and rupture velocities (1–4 km/s; Scholz, 2002).

The observed transition from ductile shear to seismic rupture is puzzling because ductile shear localization suggests strain softening (e.g., Jin et al., 1998), while seismic rupture indicates a substantial stress accumulation. The association of pseudotachylyte and mylonite has been observed in many localities (e.g., Sibson, 1980; Passchier, 1982; White, 1996, 2004), for which different interpretations have been proposed (e.g., Sibson, 1980; Hobbs et al., 1986; White, 1996, 2004; Kelemen and Hirth, 2007). Because of the occurrence of amphibole in the neoblasts in host mylonite and the ubiquity of dolomite in the pseudotachylyte, we infer that fluid had evolved in composition during the preseismic ductile shearing and played an important role in such a rheological transition.

Fluid Chemistry Evolution and Consequences on Rock Strength

We suppose that a fluid introduced in the shear zone originally contained CO_2 as well as H_2O. The introduction of fluid and the progress of shear deformation may have occurred concomitantly and cooperatively because metamorphic reactions and recrystallization would enhance the rock ductility (e.g., White and Knipe, 1978). The formation of amphibole in metamorphic reactions consumes H_2O, making the residual fluid progressively enriched with CO_2 if the supply of a new fluid is limited or delayed. The CO_2 enrichment in the fluid would reduce the connectivity of the fluid because of the increase of fluid dihedral angle, thereby reducing the permeability (Watson and Brenan, 1987; Riley and Kohlstedt, 1990), thus impeding an external supply of additional H_2O-rich fluid. The fluid-circulating system thus becomes unstable and will eventually become closed due to the permeability loss. Once the system becomes closed, it will continue being so until some catastrophic structural change such as rupture occurs. The ubiquity of dolomite in the pseudotachylyte can suggest that the activity of H_2O was not internally buffered during the preseismic metamorphism. The reduction of H_2O activity will cause a hardening of olivine due to reduction of point defects (Karato et al., 1986). Thus the reaction-controlled chemical evolution of the fluid from H_2O-rich to CO_2-rich likely results in a strain hardening in the shear zone.

Ambient Conditions During Deformation

The temperature of the preseismic deformation was estimated to be ~800 °C by applying the Ca-Mg exchange pyroxene geothermometer (Taylor, 1988) to the microprobe analyses of the neoblastic pyroxenes in the host mylonite (Table DR1), and we consider this representing the ambient condition of the seismic event. Given the grain size (<2 m) of the mylonitized pseudotachylyte vein, too small for microprobe analyses, we used the dolomite-enstatite equilibria to estimate the *postseismic* ambient conditions. The dolomite-enstatite stability field is bounded at high temperatures by the decarbonate reaction (Fig. 4) (Brey et al., 1983),

$$\text{enstatite} + \text{dolomite} = \text{diopside} + \text{forsterite} + CO_2, \quad (1)$$

and at the low temperature by the reaction,

$$\text{diopside} + \text{magnesite} = \text{enstatite} + \text{dolomite}. \quad (2)$$

Note that reaction 2 is a CO_2-conserving reaction, and therefore it is independent of the activity of CO_2. Considering the variability of the activities of H_2O and CO_2, it is conceivable that the preseismic and postseismic recrystallizations share the same *P-T* regime. It follows that pseudotachylytes were produced at ambient conditions of ~800 °C and 0.7–1.1 GPa (Fig. 4). Given the exhumation history of the Balmuccia peridotite, this *P-T* estimate would correspond to continental, lower-crust, or, probably (e.g., Fig. 11 in Handy and Stünitz, 2002), upper-mantle deformation conditions.

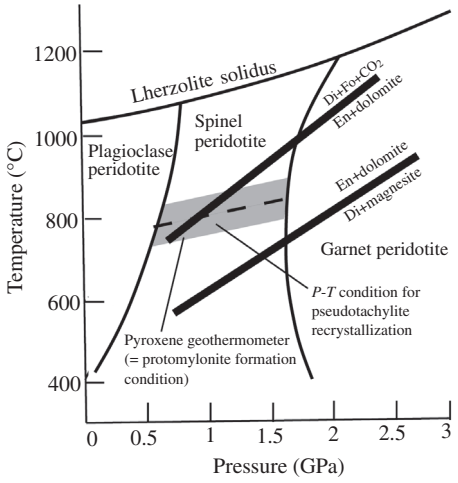

Figure 4. Ambient *P-T* condition for deformation of the wall rock (gray band) and of the pseudotachylyte vein (area between thick lines; see text). Temperature obtained by pyroxene geothermometer is indicated by a dashed line (the gray band includes the error). Lherzolite facies boundaries (for CaO-MgO-Al_2O_3-SiO_2 system) after Gasparik (1984). Reaction lines of carbonate (see text) after Brey et al. (1983). Di—diopside; En—enstatite; Fo—forsterite.

CONCLUSIONS

Microstructural and mineralogical observations of an ultramafic mylonitized pseudotachylyte have provided information about the seismic cycle at lower-crust or upper-mantle conditions. The cycle includes initial fluid-assisted ductile shear localization (producing host mylonite), followed by a seismic slip (producing pseudotachylyte), and further ductile shear (producing ultramylonite). All these deformation events took place in the spinel-lherzolite stability field (~800 °C and 0.7–1.1 GPa). Such high-temperature deformation conditions preclude the formation or the preservation of glasses or quench textures typically observed in more common shallow-seated pseudotachylytes, which makes the recognition of pseudotachylytes difficult in high-grade terrains. Identification and detailed study of such mylonitized pseudotachylytes remains an important task for further study of earthquake mechanics in the upper mantle.

ACKNOWLEDGMENTS

We thank Greg Hirth, Joe Clancy White, and an anonymous reviewer for their detailed comments to improve the manuscript. Ueda, Obata, and Di Toro thank T. Shimamoto and A. Tsutsumi for many discussions and encouragements, and T. Hirose for supplying some critical sample and field information. Di Toro thanks O. Fabbri and G. Pennacchioni for field support; Ueda and Obata thank H. Nagahara for the use of FE-SEM at Tokyo, and H. Yoshida for his technical assistance. Obata thanks F. Seifert and Bayerisches Geoinstitut (University of Beyreuth) for financially supporting the fieldwork in 1993. Kanagawa was supported by Japan Society for the Promotion of Science grant 17340159, and Di Toro by Progetti di Rilevante Interess Nazionale grant 2005044945 and a Progetti di Eccellenza Fondazion Cassa di Risparmio di Padove e Rovigo (CARIPARO) grant.

REFERENCES CITED

Andersen, T.B., and Austrheim, H., 2006, Fossil earthquakes recorded by pseudotachylytes in mantle peridotite from the Alpine subduction complex of Corsica: Earth and Planetary Science Letters, v. 242, p. 58–72, doi: 10.1016/j.epsl.2005.11.058.

Brey, G., Brice, W.R., Ellis, D.J., Green, D.H., Harris, K.L., and Ryabchikov, I.D., 1983, Pyroxene-carbonate reactions in the upper mantle: Earth and Planetary Science Letters, v. 62, p. 63–74, doi: 10.1016/0012-821X(83)90071-7.

Bridgman, P.W., 1936, Shearing phenomena at high pressure of possible importance for geology: Journal of Geology, v. 44, p. 653–669.

Carter, N.L., and Avé Lallemant, H.G., 1970, High temperature flow of dunite and peridotite: Geological Society of America Bulletin, v. 81, p. 2181–2202, doi: 10.1130/0016-7606(1970)81[2181:HTFODA]2.0.CO;2.

Di Toro, G., Nielsen, S., and Pennacchioni, G., 2005, Earthquake rupture dynamics frozen in exhumed ancient faults: Nature, v. 436, p. 1009–1012, doi: 10.1038/nature03910.

Gasparik, T., 1984, Two-pyroxene thermobarometry with new experimental data in the system CaO-MgO-Al_2O_3-SiO_2: Contributions to Mineralogy and Petrology, v. 87, p. 87–97, doi: 10.1007/BF00371405.

Griggs, D., and Handin, J., 1960, Observations on fracture and a hypothesis of earthquakes: Geological Society of America Memoir 79, p. 343–373.

Handy, M.R., and Stünitz, H., 2002, Strain localization by fracturing and reaction weakening—A mechanism for initiating exhumation of subcontinental mantle beneath rifted margins, *in* de Meer, S., et al., eds., Deformation mechanisms, rheology and tectonics: Current status and future perspectives: The Geological Society of London Special Publication 200, p. 387–407.

Handy, M.R., Franz, L., Heller, F., Janott, B., and Zurbriggen, R., 1999, Multistage accretion and exhumation of the continental crust (Ivrea crustal section, Italy and Switzerland): Tectonics, v. 18, p. 1154–1177, doi: 10.1029/1999TC900034.

Hobbs, B.E., Ord, A., and Teyssier, C., 1986, Earthquakes in the ductile regime?: Pure and Applied Geophysics, v. 124, p. 309–335, doi: 10.1007/BF00875730.

Jin, D., Karato, S., and Obata, M., 1998, Mechanisms of shear localization in the continental lithosphere: Inference from the deformation microstructures of peridotites from the Ivrea zone, northwestern Italy: Journal of Structural Geology, v. 20, p. 195–209, doi: 10.1016/S0191-8141(97)00059-X.

Jung, H., and Karato, S., 2001, Water-induced fabric transitions in olivine: Science, v. 293, p. 1460–1463, doi: 10.1126/science.1062235.

Kanamori, H., Anderson, D.L., and Heaton, T.H., 1998, Frictional melting during the rupture of the 1994 Bolivian earthquake: Science, v. 279, p. 839–842, doi: 10.1126/science.279.5352.839.

Karato, S., Paterson, M.S., and Fitz Gerald, J.D., 1986, Rheology of synthetic olivine aggregates—Influence of grain size and water: Journal of Geophysical Research, v. 91, p. 8151–8176, doi: 10.1029/JB091iB08p08151.

Kelemen, P.B., and Hirth, G., 2007, A periodic shear-heating mechanism for intermediate-depth earthquakes in the mantle: Nature, v. 446, p. 787–790, doi: 10.1038/nature05717.

Obata, M., and Karato, S., 1995, Ultramafic pseudotachylite from the Balmuccia peridotite, Ivrea-Verbano zone, northern Italy: Tectonophysics, v. 242, p. 313–328, doi: 10.1016/0040-1951(94)00228-2.

Passchier, C.W., 1982, Pseudotachylyte and the development of ultramylonite bands in the Saint-Barthelémy Massif, French Pyrenees: Journal of Structural Geology, v. 4, p. 69–79, doi: 10.1016/0191-8141(82)90008-6.

Riley, G.N., Jr., and Kohlstedt, D.L., 1990, Melt migration in a silicate liquid-olivine system: An experimental test of compaction theory: Geophysical Research Letters, v. 17, no. 12, p. 2101–2104, doi: 10.1029/GL017i012p02101.

Rivalenti, G., Garuti, G., Rossi, A., Siena, F., and Sinigoi, S., 1981, Existence of different peridotite types and of a layered igneous complex in the Ivrea zone of the western Alps: Journal of Petrology, v. 22, p. 127–153.

Schmid, R., and Wood, B.J., 1976, Phase relationships in granulitic metapelites from the Ivrea-Verbano zone (northern Italy): Contributions to Mineralogy and Petrology, v. 54, p. 255–279, doi: 10.1007/BF00389407.

Scholz, C.H., 2002, The mechanics of earthquakes and faulting (2nd edition): Cambridge, UK, Cambridge University Press, 471 p.

Shervais, J.W., 1979, Thermal emplacement model for the alpine lherzolite massif at Balmuccia, Italy: Journal of Petrology, v. 20, p. 795–820.

Sibson, R.H., 1975, Generation of pseudotachylyte by ancient seismic faulting: Geophysical Journal of the Royal Astronomical Society, v. 43, p. 775–794.

Sibson, R.H., 1980, Transient discontinuities in ductile shear zones: Journal of Structural Geology, v. 2, p. 165–171.

Sinigoi, S., Comin-Chiaramonti, P., Demarchi, G., and Siena, F., 1983, Differentiation of partial melts in the mantle: Evidence from the Balmuccia peridotite, Italy: Contributions to Mineralogy and Petrology, v. 82, p. 351–359, doi: 10.1007/BF00399712.

Taylor, W.R., 1988, An experimental test of some geothermometer and geobarometer formulations: Neues Jahrbuch für Mineralogie, v. 172, p. 381–408.

Watson, E.B., and Brenan, J.M., 1987, Fluids in the lithosphere, 1: Experimentally determined wetting characteristics of CO_2-H_2O fluids and their implications for fluid transport, host-rock physical properties, and fluid inclusion formation: Earth and Planetary Science Letters, v. 85, p. 497–515, doi: 10.1016/0012-821X(87)90144-0.

White, J.C., 1996, Transient discontinuities revisited: Pseudotachylyte, plastic instability and the influence of low pore fluid pressure on deformation processes in the mid-crust: Journal of Structural Geology, v. 18, p. 1471–1486.

White, J.C., 2004, Instability and localization of deformation in lower crust granulites, Minas fault zone, Nova Scotia, Canada: The Geological Society of London Special Publication 224, p. 25–37, doi: 10.1144/GSL.SP.2004.224.01.03.

White, S.H., and Knipe, R.J., 1978, Transformation- and reaction-enhanced ductility in rocks: The Geological Society of London Journal, v. 135, p. 513–516.

Manuscript received 3 January 2008
Revised manuscript received 19 April 2008
Manuscript accepted 22 April 2008

Printed in USA